



Chemokine receptor-4 targeted PET/CT with ^{68}Ga -Pentixafor in assessment of newly diagnosed multiple myeloma: comparison to ^{18}F -FDG PET/CT

Qingqing Pan^{1,2} · Xinxin Cao³ · Yaping Luo^{1,2} · Jian Li³ · Jun Feng³ · Fang Li^{1,2}

Received: 3 July 2019 / Accepted: 7 November 2019 / Published online: 27 November 2019
© Springer-Verlag GmbH Germany, part of Springer Nature 2019

Abstract

Purpose ^{18}F -FDG PET/CT has some limitations in the evaluation of multiple myeloma (MM). Since chemokine receptor-4 is overexpressed in MM, we perform a prospective cohort study to compare the performance of ^{68}Ga -Pentixafor and ^{18}F -FDG PET/CT in newly diagnosed MM.

Methods Thirty patients with newly diagnosed MM were recruited. All patients underwent ^{68}Ga -Pentixafor and ^{18}F -FDG PET/CT within 1 week after enrollment. A positive PET/CT was defined as the presence of focal PET-positive lesions in bone marrow or diffuse bone marrow patterns (uptake > liver). Bone marrow uptake values in ^{68}Ga -Pentixafor and ^{18}F -FDG PET/CT (total bone marrow glycolysis [TBmG_{FDG}], total bone marrow uptake with ^{68}Ga -Pentixafor [TBmU_{CXCR4}], total bone marrow volume [TBmV], SUVmean, and SUVmax) were obtained by drawing total bone marrow volume of interest on PET/CT. The positive rates of the PET/CT scans were statistically compared, and the correlation between quantitative bone marrow uptake values and clinical characteristics, laboratory findings, and staging was analyzed.

Results ^{68}Ga -Pentixafor PET/CT had a higher positive rate than ^{18}F -FDG PET/CT in recruited patients (93.3 vs. 53.3%, $p = 0.0005$). In quantitative analysis, bone marrow uptake values in ^{68}Ga -Pentixafor (TBmU_{CXCR4}, SUVmax, and SUVmean) were positively correlated with end organ damage, staging, and laboratory biomarkers related to tumor burden including serum β 2-microglobulin, serum free light chain, and 24-h urine light chain ($p < 0.05$). In ^{18}F -FDG PET/CT, only the SUVmean of total bone marrow was positively correlated with serum free light chain and 24-h urine light chain ($p < 0.05$).

Conclusions ^{68}Ga -Pentixafor PET/CT is promising in assessment of newly diagnosed MM.

Trial registration number NCT 03436342

Keywords Multiple myeloma · CXCR4 · ^{68}Ga -Pentixafor · PET/CT

Qingqing Pan and Xinxin Cao contributed equally to this work.

This article is part of the Topical Collection on Hematology

Electronic supplementary material The online version of this article (<https://doi.org/10.1007/s00259-019-04605-z>) contains supplementary material, which is available to authorized users.

✉ Yaping Luo
luoyaping@live.com

Qingqing Pan
pqqlvay@126.com

Xinxin Cao
caoxinxin@126.com

- ¹ Department of Nuclear Medicine, Chinese Academy of Medical Sciences and Peking Union Medical College Hospital, Wangfujing, Dongcheng District, 100730 Beijing, People's Republic of China
- ² Beijing Key Laboratory of Molecular Targeted Diagnosis and Therapy in Nuclear Medicine, Wangfujing, Dongcheng District, 100730 Beijing, People's Republic of China
- ³ Department of Hematology, Chinese Academy of Medical Sciences and Peking Union Medical College Hospital, Wangfujing, Dongcheng District, 100730 Beijing, People's Republic of China

Multiple myeloma (MM) is a malignant disease characterized by neoplastic proliferation of plasma cells in bone marrow producing monoclonal immunoglobulin. Myeloma tumor burden is a key factor for prognosis, usually assessed by serum β 2-microglobulin, M-protein, serum and urine-free light chain, and the percentage of plasma cell infiltrates in bone marrow. Imaging modalities are usually used to detect bone marrow involvement, lytic bone destructions, and extramedullary disease [1]. ^{18}F -FDG PET/CT has an impact on the work up of MM: the ability to distinguish between metabolically active and inactive disease is preferred to monitor the effect of therapy in MM; the presence of more than 3 focal lesions detected by ^{18}F -FDG PET/CT at baseline is a negative prognostic value in overall and event-free survival [1, 2]. Measurement of metabolic tumor burden on ^{18}F -FDG PET/CT has also been used in the prediction of prognosis in myeloma patients [3–5]. However, the false-negative FDG uptake [6–8] due to the loss of hexokinase-2 expression in MM [9] and false-positive lesions due to fractures, inflammatory or reparative changes in bones, recent chemotherapy or use of growth factors, and MM-related anemia [2, 10] hamper the assessment of the extent of disease and staging of MM with ^{18}F -FDG PET/CT.

Chemokine receptor-4 (CXCR4) has been described to play a pivotal role in tumor growth, progression, invasiveness, and metastasis. Overexpression of CXCR4 has been reported in more than 30 different tumors, including MM [11]. ^{68}Ga -Pentixafor, a novel PET tracer with high affinity for CXCR4, has recently been introduced in MM [11–13]. In 2 clinical studies on advanced and heavily pre-treated MM, ^{68}Ga -Pentixafor was superior or equal to ^{18}F -FDG for detecting myeloma lesions in 63–86% of cases [11, 12]. Thus, we wonder if ^{68}Ga -Pentixafor can better assess the tumor burden of MM compared with ^{18}F -FDG. Herein, we performed a prospective cohort study to compare the diagnostic performance of ^{68}Ga -Pentixafor and ^{18}F -FDG PET/CT in newly diagnosed MM, and then to analyze the quantitative uptake values in ^{68}Ga -Pentixafor and ^{18}F -FDG PET/CT in correlation with clinical characteristics, laboratory findings, and staging.

Methods

Study design and patients

This prospective cohort study was approved by the institutional review board of PUMCH (IRB protocol #ZS-1113) and registered at [Clinicaltrials.gov](https://clinicaltrials.gov) (NCT 03436342). To compare differences between imaging techniques, the primary endpoint was the positive rate of ^{68}Ga -Pentixafor and ^{18}F -FDG PET/CT for MM at initial diagnosis; the secondary endpoint was the correlation between quantitative measurements in both

^{68}Ga -Pentixafor and ^{18}F -FDG PET/CT and clinical characteristics, biochemical investigations, and staging of MM. On the basis of reviewing the detection rate of ^{18}F -FDG in newly diagnosed MM in our hospital, we expected that at least 25% increased positive rate with ^{68}Ga -Pentixafor would be clinically significant. With a power of 80% and α of 0.05, we planned to enroll 30 patients.

A total of 30 patients with newly diagnosed MM according to the revised International Myeloma Working Group criteria [14] in the Department of Hematology of Peking Union Medical College Hospital were consecutively recruited from January 2018 to May 2019. Relapsed MM, solitary plasmacytoma, or patients received chemotherapeutic regimens before PET/CT scans were excluded. Written informed consent was obtained from each patient. The clinical history and laboratory test results related to MM were recorded at enrollment. Patients were then referred for ^{18}F -FDG and ^{68}Ga -Pentixafor PET/CT that were carried out within 1 week after enrollment. The imaging characteristics were analyzed and quantitative parameters were measured afterwards.

PET/CT imaging

The DOTA-CPCR4-2 peptide was purchased from CSBio Co (CA 94025, USA). The radiolabeling of ^{68}Ga -Pentixafor was performed manually before injection according to the procedures as previously published [15]. ^{18}F -FDG was synthesized in house with an 11 MeV cyclotron (CTI RDS 111, Siemens, Germany).

The PET scans were performed on dedicated PET/CT scanners (Biograph64 Truepoint TrueV, Siemens, Germany; Polestar m660, SinoUnion, China) from the tip of the skull to the middle thigh. In 21 patients, PET/CT scans of the same patient were performed on the same scanner; 9 patients underwent PET/CT scans with different scanners. For ^{18}F -FDG PET/CT, patients fasted for over 6 h, and the blood glucose levels were monitored (4.2–7.5 mmol/L) prior to an injection of ^{18}F -FDG (5.55 MBq/kg). The PET/CT images (2 min/bed) were acquired with an uptake time of 71.2 ± 15.6 min (range 40–95 min). For ^{68}Ga -Pentixafor PET/CT, imaging was performed (2–4 min/bed) with an uptake time of 55.5 ± 17.6 min (range 30–90 min) after injection of 92.4 ± 31.6 MBq (range 40.7–170.2 MBq) ^{68}Ga -Pentixafor. All patients underwent unenhanced low-dose CT (120 kV, 30–50 mAs) for attenuation correction and anatomical reference. The acquired data were reconstructed using the ordered subset expectation maximization method (Siemens Biograph 64: 2 iterations, 8 subsets, Gaussian filter, image size 168*168; SinoUnion Polestar: 2 iterations, 10 subsets, Gaussian filter, image size 192*192).

Image analysis

Visual analysis

Two experienced nuclear medicine physicians (YL and QP) visually assessed PET/CT images and were in consensus for the image interpretation. The distribution and intensity of bone marrow uptake, the presence and sites of focal PET positive bone marrow lesions (defined as circumscribed focus ≥ 5 mm with increased radioactivity compared with background uptake in bone marrow, and not caused by fracture), osteolytic lesions, fractures, extramedullary, and paramedullary disease were recorded. For ^{18}F -FDG, the intensity of the bone marrow uptake and uptake in other lesions was based on the 5-point Deauville score scale, which is widely used in lymphoma and recently introduced in a new visual descriptive criterion of MM [10, 16]. For ^{68}Ga -Pentixafor, the intensity of bone marrow uptake was classified as mild, moderate, and intense with the liver and spleen taken as the reference (mild uptake \leq liver; moderate liver $<$ uptake \leq spleen; intense uptake $>$ spleen). A positive scan was defined as the presence of focal PET positive bone marrow lesions or diffuse bone marrow patterns (homogeneous bone marrow uptake) with the following interpretation criteria: for ^{18}F -FDG, a score of 4 for the bone marrow uptake was set a positive cutoff based on the high interobserver concordance in a study on the visual descriptive criterion of MM [16]; for ^{68}Ga -Pentixafor, moderate or intense uptake was defined as being positive.

Quantitative analysis

To measure values of the whole-body tumor burden, PET/CT data were transferred in DICOM format to MIM workstation (version 6.6.11, MIM Software, USA). In ^{18}F -FDG PET/CT, whole-body tumor burden is usually measured as total lesion glycolysis and metabolic tumor volume, in which tumor contours are segmented with a SUV cutoff or semiautomatically delineated by using a threshold of certain percentage of SUVmax within the lesion. Such measurements are applicable in solid tumors and hematological malignancies with focal lesions; however, it is not feasible in measuring diffuse bone marrow infiltration, which is usually the case in MM. As MM predominantly affects bone marrow, we measured the total bone marrow glycolysis in ^{18}F -FDG (TBmG_{FDG}) and total bone marrow uptake in ^{68}Ga -Pentixafor PET/CT (TBmU_{CXCR4}) with the following procedures. Briefly, the technique consisted of drawing a rectangular semiautomatic volume of interest (VOI) in the whole body on PET/CT. Subsequently, the software automatically generated whole-body skeleton VOI surrounding regions with a CT attenuation value of 200 HU or greater, followed by automatic expansion, and then contraction of the VOI to include all the aspects of the bone and bone marrow. Then the VOI was manually adjusted to exclude extraosseous calcification and other high density focus to obtain

the total bone marrow VOI. In cases with paramedullary or extramedullary disease, VOIs of extraosseous disease were manually drawn and added to the final VOI. Afterward, volumetric parameters of total bone marrow uptake (with extraosseous disease) were automatically obtained from the statistics generated with the final volumetric extraction, including SUVmean, SUVmax, total bone marrow volume (TBmV), TBmG_{FDG}, and TBmU_{CXCR4} (determined as a product of SUVmean \times TBmV). Figure 1 is an example of the calculation of the TBmG_{FDG} in ^{18}F -FDG PET/CT.

Statistical analysis

Statistical analyses were done with the SPSS Statistics software (version 22.0, IBM SPSS Inc.). The McNemar's test was used to statistically compare the positive rates of ^{68}Ga -Pentixafor and ^{18}F -FDG PET/CT. Comparison of numerical data of 2 groups was performed using Student *t* test for data with normal distribution and Wilcoxon rank sum test for skewed data; one-way analysis of variance (for data with normal distribution) or Kruskal-Wallis test (for skewed data) was used for comparison of more than 2 group means. For correlation analyses, Pearson's correlation coefficients (for data with normal distribution) or Spearman's rank correlation coefficients (for skewed data) were conducted. A *p* value < 0.05 was considered statistically significant.

Results

Clinical characteristics

Thirty patients with newly diagnosed MM (19 male, 11 female; age, 59.1 ± 9.8 year, range 33–77 year) were enrolled in this study. The type of M protein included IgG in 11 patients, IgA in 10 patients, and light chain in 9 patients. The median proportion of infiltrated plasma cells found from bone marrow aspiration was 24.0% (range, 4.0–93.5%).¹ Regarding the end-organ damage, hypercalcemia and renal failure were found in 4/30 (13.3%) and 8/30 (26.7%) patients, respectively; 18/30 (60.0%) patients had anemia. Lytic bone lesions were found in 20/30 (66.7%) patients, and 10/30 (33.3%) patients had bone fractures in vertebra, sternum, rib, and pubis. One patient (patient 7) had secondary amyloidosis due to MM affecting the gastrointestinal tract, myocardium, and skin. According to the International Staging System for MM [17], 7 patients were classified as stage I, and 4 patients were stage II; 19 patients had stage III disease. High-risk cytogenetics

¹ Two patients (patients 2 and 5) had bone marrow plasma cells lower than 10%. Patient 2 was presented with biopsy-proven plasmacytoma in T3 vertebra. In patient 5, the plasma cells in bone marrow core biopsy were 70% (however, 4% in bone marrow aspirates).

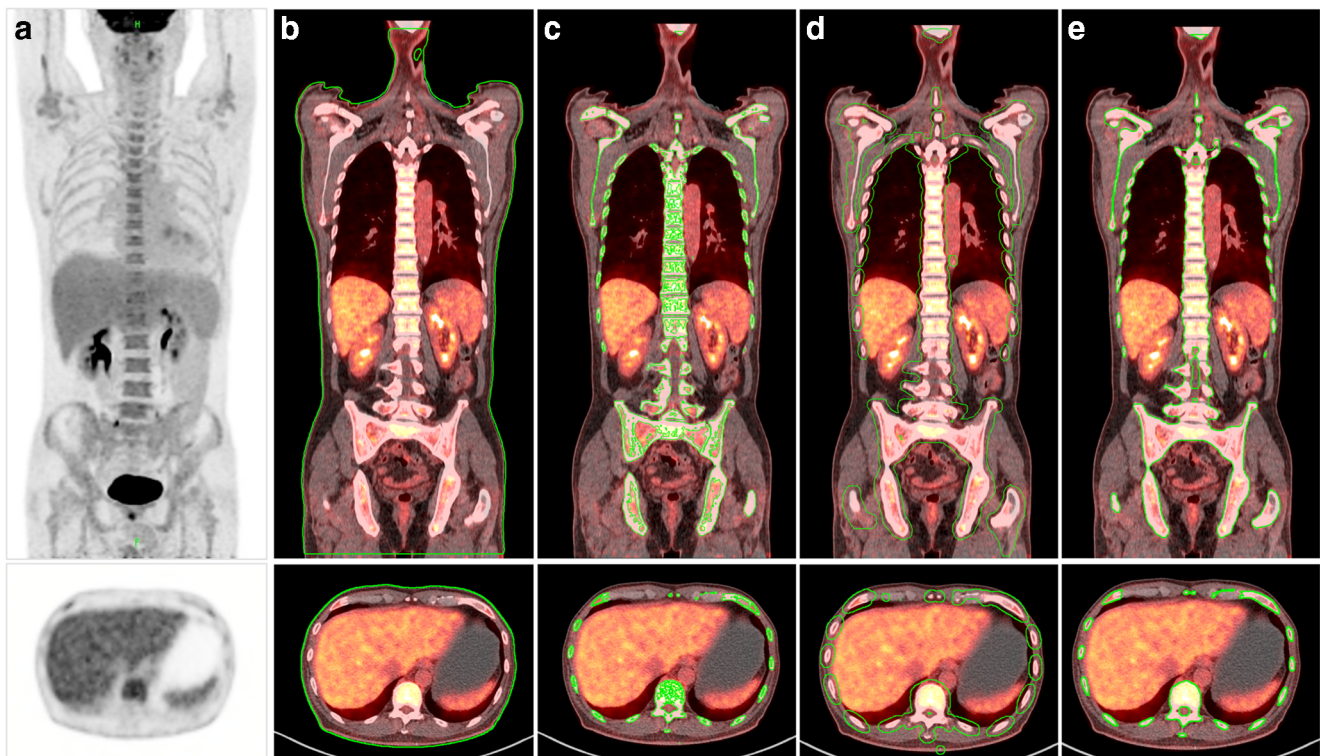


Fig. 1 Calculation of TBm_{GFDG} and TBmV on ¹⁸F-FDG PET/CT. **a** ¹⁸F-FDG-PET of patient 3 with diffuse bone marrow pattern (uptake score 4). **b** Semiautomatic VOI is drawn in whole-body image. **c** With threshold density > 200 HU on CT, all soft tissue is subtracted. Notice that some

part of bone marrow is also subtracted. **d** With automatic expansion and then **e** contraction of the VOI, the whole-body bone marrow VOI is automatically generated. Statistics demonstrate bone marrow SUV_{mean} 1.4, SUV_{max} 5.1, TBmV 3903.7 ml, and TBm_{GFDG} 5611.0

(defined by the presence of del(17p), t(4;14), and t(14;16) [18]) was documented in 13/25 (52.0%) patients with fluorescence in situ hybridization test. Flow cytometry of bone marrow was performed in 2 patients, and both patients had CXCR4-positive myeloma (CD184+/CD138+ cells; 91.4% and 100%, respectively). The clinical characteristics and biochemical investigations are summarized in Table 1.

Comparison of ⁶⁸Ga-Pentixafor and ¹⁸F-FDG PET/CT

With the formerly described visual assessment criteria, ⁶⁸Ga-Pentixafor PET/CT was visually positive in 28/30 (93.3%) patients, while ¹⁸F-FDG PET/CT was positive in 16/30 (53.3%) patients. The diagnostic performance of ⁶⁸Ga-Pentixafor PET/CT and ¹⁸F-FDG PET/CT in newly diagnosed MM is shown in Tables 1 and 2.

Bone marrow involvement

In ⁶⁸Ga-Pentixafor PET/CT, 18 patients had intense radioactivity in the bone marrow with a SUV_{max} of 17.0 ± 15.1 (range 6.1–74.5); 10 patients showed moderate uptake in the bone marrow (SUV_{max} 5.8 ± 1.3 , range 4.4–8.2). The remaining 2 patients had mild ⁶⁸Ga-Pentixafor uptake in the bone marrow that was classified as negative according to the visual assessment criteria in this study, and were also negative

of FDG uptake, and these 2 patients had a low serum β 2-microglobulin level. In ¹⁸F-FDG PET/CT, 15 patients had bone marrow uptake with a score ≥ 4 (SUV_{max} 7.1 ± 4.9 , range 2.6–23.5), and the remaining 15 patients had bone marrow intensity with a score of 3 (in 2 patients) and a score of 2 (in 13 patients).

According to ⁶⁸Ga-Pentixafor and ¹⁸F-FDG PET/CT, 17/30 (56.7%) patients showed diffuse bone marrow patterns with homogeneous radioactivity throughout the axial and appendicular skeleton without focal lesions: 11 patients had visually much higher uptake of ⁶⁸Ga-Pentixafor in the bone marrow than ¹⁸F-FDG uptake (mean SUV_{max}, 7.8 ± 3.5 vs. 2.5 ± 0.9 , $p < 0.01$) (example in Fig. 2a); in the remaining 6 patients, the bone marrow intensity in ⁶⁸Ga-Pentixafor and ¹⁸F-FDG PET was visually comparable. ⁶⁸Ga-Pentixafor showed significantly higher sensitivity in diffuse bone marrow pattern than those in ¹⁸F-FDG (Table 2).

Focal bone marrow lesions were detected in 13/30 (43.3%) patients, and all of them had more than 10 focal lesions detected by dual-tracer PET/CT. All of the focal bone marrow lesions showed osteolytic changes. Regarding the detectability of intramedullary focal lesions, 12 patients were detected by ⁶⁸Ga-Pentixafor and 9 by ¹⁸F-FDG (mean SUV_{max}, 20.4 ± 17.4 vs. 8.9 ± 5.6 , $p < 0.05$) (Table 2). ⁶⁸Ga-Pentixafor PET demonstrated much more focal lesions with more intense uptake in 6 patients than ¹⁸F-FDG PET in these individuals, and

Table 1 Patients’ clinical characteristics, biochemical investigations, and PET/CT diagnosis

No	Age/sex	MM type	ISS	Cytogenetics	M-pro (g/L)	β2MG (mg/L)	sFLC (mg/L)	24-h urine LC (mg)	PET/CT diagnosis	
									CXCR4	FDG
1	74/M	LC-λ	III	high risk	1.7	7.6	10,404.8 (λ)	67,935 (λ)	P	N
2	66/F	IgG-λ	III	n/a	1.6	6.5	825 (λ)	11,466 (λ)	P*	N
3	55/M	IgG-κ	III	n/a	71.7	12.1	n/a	n/a	P	P
4	61/F	IgA-κ	I	n/a	17.3	2.1	457.5 (κ)	108.9 (κ)	N	N
5	66/F	LC-κ	III	high risk	0.8	27.7	1590 (κ)	22,560 (κ)	P*	P*
6	52/M	LC-κ	I	other	0	3.2	1055 (κ)	4770 (κ)	P*	P
7	67/M	LC-κ	III	other	1.5	11.5	5850 (κ)	5473 (κ)	P	P
8	61/F	LC-κ	II	high risk	0	4.9	1765 (κ)	10,512 (κ)	P*	P*
9	33/F	LC-κ	II	other	0.4	3.9	5700 (κ)	4361 (κ)	P*	P*
10	58/M	IgA-λ	II	high risk	3.9	3.5	8.8 (λ)	0	P	N
11	71/M	IgA-κ	III	high risk	26.5	9.3	30.2 (κ)	127 (κ)	P	N
12	69/F	IgG-κ	I	high risk	25.7	3.0	19.5 (κ)	0	N	N
13	43/M	LC-λ	III	other	2.5	10.8	7600 (λ)	33,375 (λ)	P	N
14	49/M	IgG-λ	III	other	76.9	5.6	n/a†	0	P	N
15	51/F	IgG-λ	III	high risk	70.8	9.4	1060 (λ)	2934 (λ)	P*	P*
16	64/M	IgA-κ	I	other	7.5	3.3	62.2 (κ)	0	P	P*
17	77/F	IgG-λ	III	other	54.9	5.8	101 (λ)	0	P	N
18	50/M	IgA-κ	III	other	32.4	7.7	977.5 (κ)	10,082 (κ)	P	P
19	60/M	IgG-λ	III	high risk	25.9	27.1	3285 (λ)	30,189 (λ)	P*	P*
20	69/M	IgG-κ	III	high risk	42.7	11.3	2050.2 (κ)	412.5 (κ)	P*	P*
21	47/M	IgA-λ	III	high risk	71.9	10.6	1000 (λ)	5290 (λ)	P	P
22	55/M	IgG-κ	III	other	1.1	10.7	4200 (κ)	867 (κ)	P	N
23	70/M	IgA-λ	II	high risk	41.9	3.0	22.5 (λ)	261 (λ)	P*	P
24	49/M	IgA-κ	III	other	42.4	15.5	84.2 (κ)	495 (κ)	P*	P*
25	54/M	LC-κ	III	high risk	13.0	35.8	178,000 (κ)	18,590 (κ)	P*	P*
26	66/M	IgA-λ	III	n/a	5.4	23.1	10,950 (λ)	9120 (λ)	P	N
27	61/M	LC-λ	III	high risk	1.1	7.8	3945 (λ)	9250 (λ)	P*	N
28	66/F	IgG-λ	I	other	23.7	2.0	193.8 (λ)	n/a	P	N
29	53/M	IgG-κ	I	n/a	9.6	1.4	16.5 (κ)	0	P	N
30	56/F	IgA-κ	I	other	38.2	2.5	342.5 (κ)	222 (κ)	P	P

MM multiple myeloma, ISS International Staging System, sFLC serum free light chain, LC light chain, n/a not applicable, P positive, N negative

*Additional focal bone marrow lesions were detected

†sFLC could not be accurately measured because of significant M protein level

4 of them had focal bone marrow lesions purely avid for ⁶⁸Ga-Pentixafor (example in Fig. 2b). Three patients were detected to have more focal lesions by ¹⁸F-FDG PET, and one patient who was pretreated by intravenous immunoglobulin was purely avid for ¹⁸F-FDG. In the remaining 4 patients, the detectability of focal bone marrow lesions and the intensity of uptake in ⁶⁸Ga-Pentixafor and ¹⁸F-FDG PET were comparable (example in Fig. 2c).

Paramedullary involvement

There was a paramedullary disease (bone related plasmacytoma) in 8/30 (26.7%) patients, which affected the soft tissues around the sternum, thoracic vertebra, ribs, and pelvis. The paramedullary disease in 3 patients had both positive ⁶⁸Ga-Pentixafor uptake and ¹⁸F-FDG avidity. In 4 patients, ⁶⁸Ga-Pentixafor PET/CT showed intense radioactivity

Table 2 Diagnostic performance of ⁶⁸Ga-Pentixafor and ¹⁸F-FDG PET/CT

	⁶⁸ Ga-Pentixafor (%)	¹⁸ F-FDG (%)	p value
PET-positive patients	28/30 (93.3)	16/30 (53.3)	0.0005*
Bone marrow involvement			
Diffuse bone marrow patterns (n = 17)	15/17 (88.2)	5/17 (29.4)	0.002*
Focal bone marrow lesions† (n = 13)	12/13 (92.3)	9/13 (69.2)	0.371
> 10 focal lesions (n = 13)	10/13 (76.9)	7/13 (53.8)	0.505
Paramedullary disease	7/30 (22.6)	4/30 (12.9)	0.375

*The difference in the positive rate between ⁶⁸Ga-Pentixafor and ¹⁸F-FDG is significant

† The patients had both focal bone marrow lesions and diffuse bone marrow involvement

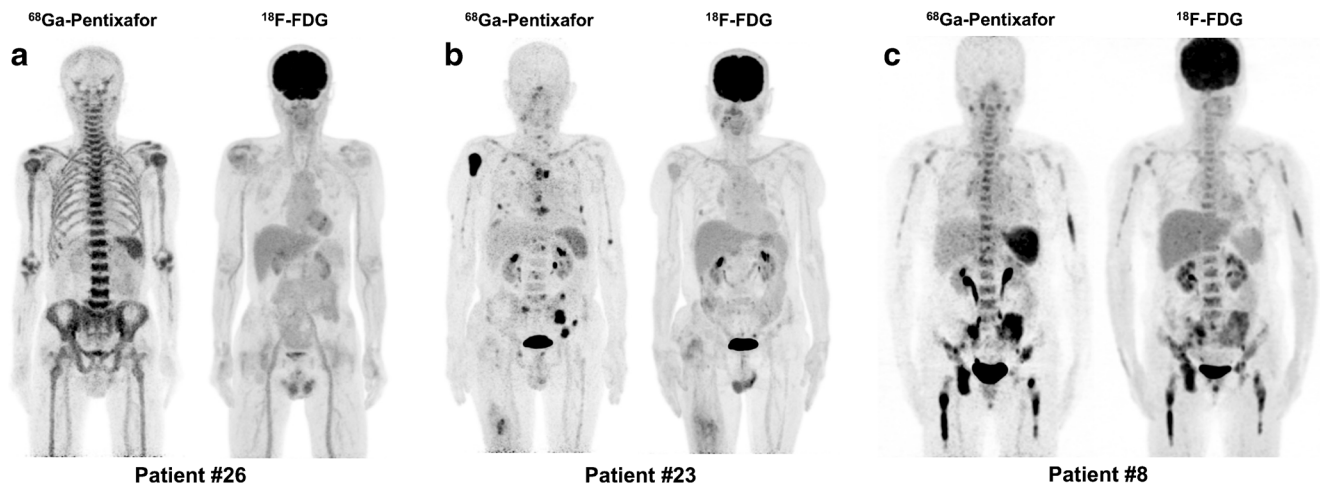


Fig. 2 Examples of ^{68}Ga -Pentixafor and ^{18}F -FDG PET in MM. **a** Patient #26 with IgA- λ MM presenting as diffuse bone marrow pattern. The bone marrow had intense ^{68}Ga -Pentixafor uptake but negative ^{18}F -FDG avidity. **b** Patient #23 with IgA- λ MM. Multiple bone marrow lesions were

shown in ^{68}Ga -Pentixafor PET but negative for FDG uptake. **c** Patient #8 with LC- κ MM. The detectability of focal bone marrow lesions and the intensity of uptake of ^{68}Ga -Pentixafor and ^{18}F -FDG PET were comparable

in the paramedullary disease, and the intensity of FDG uptake was scored as 2–3 in these lesions. The remaining one patient had FDG-avid paramedullary disease that was negative of ^{68}Ga -Pentixafor uptake. No authentic extramedullary disease was detected in the recruited patients.

Quantitative PET/CT parameters and clinical features

The TBmV measured in ^{68}Ga -Pentixafor and ^{18}F -FDG PET/CT in each patient were not significantly different (paired *t* test, $p = 0.44$; Supplement Fig. 1). Quantitative PET/CT parameters including TBmU_{CXCR4}, TBmG_{FDG}, SUVmean, and SUVmax of total bone marrow in both ^{68}Ga -Pentixafor and ^{18}F -FDG PET/CT and clinical features were statistically analyzed (Table 3 and Fig. 3).

End-organ damage

The end-organ damage of MM known as hypercalcemia, renal failure, anemia, and destructive bone lesions (CRAB criteria) was scored according to the number of MM-defining events in each patient: score 0, no end-organ damage; score 1, 1 damaged end-organ; score 2, 2 damaged end-organs; score 3, 3 damaged end-organs; score 4, 4 damaged end-organs. The quantitative parameters measured in ^{68}Ga -Pentixafor PET/CT including TBmU_{CXCR4}, SUVmean, and SUVmax of the bone marrow were positively correlated with the scores of end-organ damage ($p < 0.01$, Table 3). No correlation was found between ^{18}F -FDG uptake values (TBmG_{FDG}, SUVmean, and SUVmax) and end-organ damage scores ($p > 0.05$, Table 3).

Laboratory findings

In ^{68}Ga -Pentixafor PET/CT, TBmU_{CXCR4}, SUVmean, and SUVmax of total bone marrow were positively correlated with serum $\beta 2$ -microglobulin, serum free light chain, and 24-h urine light chain ($p < 0.05$, Table 3). The above ^{68}Ga -Pentixafor uptake values were also negatively correlated with hemoglobin ($p < 0.05$, Table 3), however not well correlated with serum albumin, M-protein, or the percentage of plasma cell infiltrates obtained from bone marrow aspiration ($p > 0.05$, Table 3). For ^{18}F -FDG PET/CT, only the SUVmean of total bone marrow was found to be positively correlated with serum free light chain (Spearman $r = 0.403$, $p = 0.033$) and 24-h urine light chain (Spearman $r = 0.395$, $p = 0.037$). ^{18}F -FDG uptake values were independent from hemoglobin, serum albumin, $\beta 2$ -microglobulin, M-protein, and the percentage of plasma cell infiltrates ($p > 0.05$, Table 3). Regarding the cytogenetic features, there was no significant difference of the quantitative measurements in both ^{68}Ga -Pentixafor and ^{18}F -FDG PET/CT between the high- and low-risk cytogenetic groups (Student *t* test, ^{68}Ga -Pentixafor, $p = 0.11$ – 0.61 ; ^{18}F -FDG, $p = 0.38$ – 0.54).

Staging

In Spearman's rank correlation test, there was a positive correlation between the ^{68}Ga -Pentixafor uptake values (TBmU_{CXCR4}, SUVmean, and SUVmax of the bone marrow) and the International Staging System for MM ($n = 30$, $p < 0.01$, Table 3); the ^{68}Ga -Pentixafor uptake values were also positively correlated with the Revised International Staging System based on the original International Staging System in conjunction with the cytogenetic findings and lactate dehydrogenase levels [18] ($n = 25$, $p < 0.05$, Table 3). Comparing

Table 3 Spearman's rank correlation test of quantitative PET/CT parameters and clinical features

Characteristics	Coefficient	⁶⁸ Ga-Pentixafor-PET			¹⁸ F-FDG-PET		
		TBmU _{CXCR4}	SUVmean	SUVmax	TBmG _{FDG}	SUVmean	SUVmax
CRAB [†]	<i>r</i>	0.54	0.52	0.52	0.25	0.27	0.29
	<i>p</i>	0.002*	0.003*	0.004*	0.185	0.147	0.126
Hb	<i>r</i>	− 0.41	− 0.55	− 0.38	− 0.12	− 0.34	− 0.11
	<i>p</i>	0.025*	0.002*	0.038*	0.529	0.065	0.54
ALB	<i>r</i>	0.008	0.007	0.007	0.06	− 0.06	0.03
	<i>p</i>	0.968	0.760	0.970	0.760	0.773	0.893
M-protein	<i>r</i>	0.04	− 0.13	− 0.12	0.05	− 0.01	− 0.04
	<i>p</i>	0.838	0.498	0.518	0.805	0.962	0.820
β2MG	<i>r</i>	0.59	0.56	0.44	0.23	0.33	0.27
	<i>p</i>	0.0008*	0.002*	0.016*	0.231	0.085	0.152
sFLC	<i>r</i>	0.54	0.62	0.45	0.26	0.403	0.19
	<i>p</i>	0.003*	0.0004*	0.018*	0.175	0.033*	0.332
24-h urine LC	<i>r</i>	0.42	0.53	0.56	0.23	0.395	0.19
	<i>p</i>	0.025*	0.004*	0.002*	0.239	0.037*	0.321
BM plasma cell %	<i>r</i>	0.32	0.25	0.34	0.17	0.09	0.13
	<i>p</i>	0.085	0.183	0.071	0.361	0.627	0.509
ISS	<i>r</i>	0.62	0.59	0.48	0.11	0.19	0.08
	<i>p</i>	0.0003*	0.0006*	0.007*	0.551	0.322	0.672
R-ISS	<i>r</i>	0.57	0.48	0.46	0.17	0.24	0.24
	<i>p</i>	0.003*	0.015*	0.020*	0.415	0.245	0.240

Hb hemoglobin, *ALB* serum albumin, *β2MG* β2-microglobulin, *sFLC* serum free light chain, *LC* light chain, *BM* bone marrow, *ISS* International Staging System, *R-ISS* Revised International Staging System

*The correlation coefficient is significant

[†] CRAB stands for the score of end-organ damage in MM: *C* hypercalcemia, *R* renal failure, *A* anemia, *B* lytic bone lesions; *score 0*, no end-organ damage; *score 1*, 1 damaged end-organ; *score 2*, 2 damaged end-organs; *score 3*, 3 damaged end-organs; *score 4*, 4 damaged end-organs

the ⁶⁸Ga-Pentixafor uptake values of each stage, there was also a significant difference with a trend of increasing uptake values towards a higher stage (Kruskal-Wallis test, International Staging System [*n* = 30], *p* < 0.01; Revised International Staging System [*n* = 25], TBmU_{CXCR4} vs. stage, *p* = 0.016; Fig. 3). ¹⁸F-FDG uptake values of bone marrow were not correlated with the stage (Table 3 and Fig. 3).

Discussion

In our study, ⁶⁸Ga-Pentixafor showed significantly higher positive rate than ¹⁸F-FDG in MM, especially in patients presenting as diffuse bone marrow patterns (88.2 vs. 29.4%, *p* = 0.002). The detectability of focal bone marrow lesions in ⁶⁸Ga-Pentixafor was superior or at least equal to that in ¹⁸F-FDG in 10/13 patients, while ¹⁸F-FDG detected more focal lesions than ⁶⁸Ga-Pentixafor in 3/13 patients. One patient who was purely avid for ¹⁸F-FDG was pretreated by intravenous immunoglobulin, which we assumed that the false negative of ⁶⁸Ga-Pentixafor uptake might be attributed to, since a

decrease of CXCR4 expression following intravenous immunoglobulin therapy was determined in a study of gene expression profiling in peripheral blood mononuclear cells [19]. In another patient with multiple small focal lesions in bone marrow, ¹⁸F-FDG detected more lesions than ⁶⁸Ga-Pentixafor did probably due to the inferior image quality of ⁶⁸Ga; moreover, 2 additional lesions were shown only on ⁶⁸Ga-Pentixafor PET in this patient. The reason of ⁶⁸Ga-Pentixafor negative focal lesions in the remaining patient was unknown. The significance of focal bone marrow lesions detected by ⁶⁸Ga-Pentixafor to the prognosis of MM needs to be clarified in further study. For the detection of paramedullary disease, 1/8 patient had CXCR4 negative lesion. As SDF-1/CXCR4 is a critical regulator of migration and homing of MM cells through the blood to bone marrow niches [20], and the loss of CXCR4 expression is associated with extramedullary disease [21], the CXCR4 negative paramedullary disease may share the same mechanism due to the manner of extramedullary invasion.

Our study determined significant positive correlations between ⁶⁸Ga-Pentixafor uptake values in total bone marrow

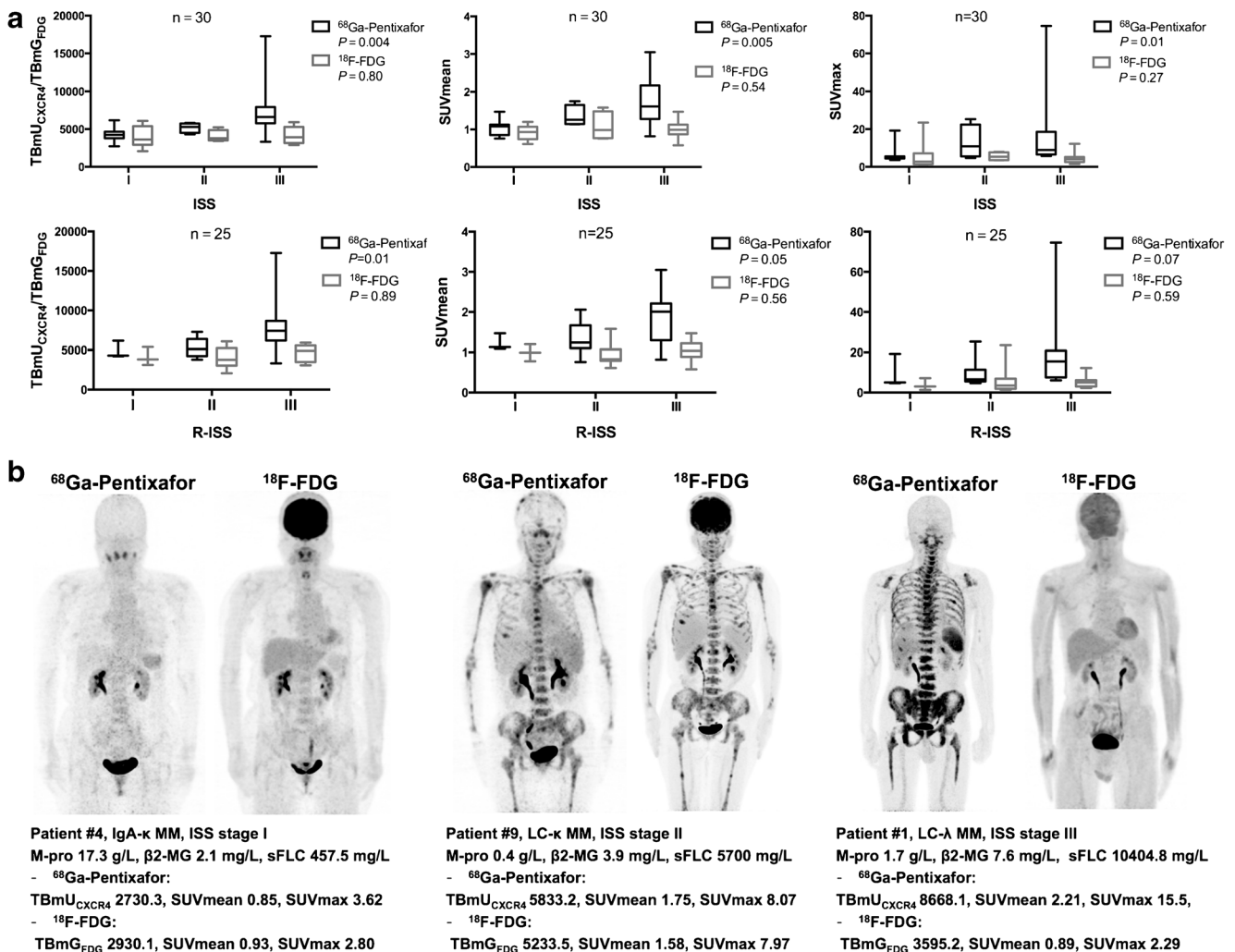


Fig. 3 **a** Box plots of comparison between bone marrow uptake values of ⁶⁸Ga-Pentixafor and ¹⁸F-FDG (TBmU_{CXCR4}/TBmG_{FDG}, SUVmean, SUVmax) and staging. The box and whiskers showed the interquartile range and the minimum to maximum range. The Kruskal-Wallis test was performed for the statistical analysis. **b** Examples of 3 patients showing

different levels of bone marrow uptake in ⁶⁸Ga-Pentixafor PET/CT correspond to stage, serum β2MG, and sFLC. The ¹⁸F-FDG uptake values of these patients were not correlated with stage. ISS International Staging System, R-ISS Revised International Staging System, β2MG β2-microglobulin, sFLC serum free light chain, LC light chain

(TBmU_{CXCR4}, SUVmax, and SUVmean) and end-organ damage, staging, and laboratory biomarkers related to tumor burden including serum β2-microglobulin, serum free light chain, and 24-h urine light chain. However, the ⁶⁸Ga-Pentixafor uptake values were not well correlated with M protein levels or the percentage of plasma cell infiltrates in bone marrow aspiration. This might be explained by the fact that M protein is not a good marker for tumor burden in light chain myeloma [22]; and the percentage of plasma cell infiltrates obtained from a single site bone marrow aspiration may not replace whole-body evaluation. For this reason, we further analyzed the correlation between M protein and ⁶⁸Ga-Pentixafor uptake values in patients excluding light chain myeloma, but the correlation was still not significant (Spearman $r = 0.21-0.29$, $p = 0.18-0.35$). We think that sample size might

be a problem and further studies are warranted to address this issue. Besides the above tumor burden markers, ⁶⁸Ga-Pentixafor uptake values were found to be negatively correlated with hemoglobin. Unlike ¹⁸F-FDG, CXCR4 expression is not regulated by erythropoietic activity in bone marrow, but is related to CXCR4-positive tumor cell infiltration and activated inflammatory cells with upregulated CXCR4 expression [11, 23–25]. As anemia is one of the common events in MM, and 60% of the recruited patients had anemia because of myeloma cell infiltration in bone marrow, we speculated that the correlation between ⁶⁸Ga-Pentixafor uptake values and hemoglobin was related to the tumor burden in bone marrow.

Our study has several limitations. First, apart from CXCR4-positive tumor cell infiltration, other activated

inflammatory cells in the bone marrow with upregulated CXCR4 expression may also cause increased bone marrow uptake [23–25]. Therefore, the $TBmU_{CXCR4}$ we measured in ^{68}Ga -Pentixafor PET/CT might not represent pure CXCR4 expression in myeloma cells, but a combination of myeloma and activated inflammatory cells with upregulated CXCR4 expression in bone marrow, if any. Moreover, the heterogeneity of PET/CT protocols (e.g., uptake time, dose, use of 2 different PET/CT scanners, and reconstruction parameters) may bias the quantitative PET/CT measurements. In addition, as we measured the quantitative values of $TBmV$, $TBmU_{CXCR4}$, and $TBmG_{FDG}$ based on CT attenuation of bones, it naturally included normal bone marrow. So, we did not perform statistical analysis on $TBmV$ and clinical characteristics. Second, we did not include MRI in our study, which is a gold standard for assessment of diffuse bone marrow involvement of the spine [2]; thus, we cannot confirm whether the 2 patients with false-negative ^{68}Ga -Pentixafor and ^{18}F -FDG scans might have more disease detected in MR. Third, we performed flow cytometry of bone marrow specimens in 2 patients and confirmed CXCR4-positive MM (both patients with intense ^{68}Ga -Pentixafor uptake in bone marrow); however, such assessments were not performed in all recruited patients. Previous studies have determined that ^{68}Ga -Pentixafor was bound with high specificity and selectivity to human CXCR4, and CXCR4 expression was correlated with cellular uptake of ^{68}Ga -Pentixafor; moreover, high levels of membranous CXCR4 expression in bone marrow were identified in myeloma patients [11, 26]. We think that these results have provided strong evidence of the mechanism of CXCR4-mediated ^{68}Ga -Pentixafor uptake in MM. Finally, considering the surface expression of CXCR4 in MM is a dynamic process influenced by chemotherapy [27, 28], we enrolled newly diagnosed MM patients that were treatment-naïve in order to avoid the heterogeneity of the study population. Therefore, the positive rate of ^{68}Ga -Pentixafor in MM was higher in our study compared with Lapa et al.'s study [12] in advanced and pre-treated patients. Furthermore, the result of the correlations between ^{68}Ga -Pentixafor uptake values in total bone marrow and tumor burden in MM in our study may not be extrapolated to relapsed MM or interim follow-up during treatment. Further studies are warranted to investigate the time- and dose-dependent manner of the influence of each chemotherapeutic drug on CXCR4 expression in MM.

In our study, ^{68}Ga -Pentixafor showed higher positive rate than ^{18}F -FDG in newly diagnosed MM. There were significant correlations between ^{68}Ga -Pentixafor uptake values in bone marrow and end-organ damage, staging, and laboratory tumor burden markers. These results indicated that ^{68}Ga -Pentixafor PET quantification might be a promising biomarker and superior to ^{18}F -FDG in assessing tumor burden of newly diagnosed MM. Further investigation is warranted to clarify whether it has an impact on patients' prognosis and survival.

Funding information This work was supported by the National Natural Science Foundation of China (81701741) and CAMS Initiative for Innovative Medicine (CAMS-I2M, 2017-I2M-3-001).

Compliance with ethical standards

Conflict of Interest The authors declare that they have no conflict of interest.

Ethical approval All procedures performed in this study involving human participants were in accordance with the ethical standards of the institutional review board of PUMCH (IRB protocol #ZS-1113).

Statement of informed consent Informed consent was obtained from all individual participants included in the study.

References

- Walker RC, Brown TL, Jones-Jackson LB, De Blanche L, Bartel T. Imaging of multiple myeloma and related plasma cell dyscrasias. *J Nucl Med*. 2012;53:1091–101. <https://doi.org/10.2967/jnumed.111.098830>.
- Cavo M, Terpos E, Nanni C, Moreau P, Lentzsch S, Zweegman S, et al. Role of (18)F-FDG PET/CT in the diagnosis and management of multiple myeloma and other plasma cell disorders: a consensus statement by the International Myeloma Working Group. *Lancet Oncol*. 2017;18:e206–e17. [https://doi.org/10.1016/s1470-2045\(17\)30189-4](https://doi.org/10.1016/s1470-2045(17)30189-4).
- Fonti R, Larobina M, Del Vecchio S, De Luca S, Fabbri C, Catalano L, et al. Metabolic tumor volume assessed by 18F-FDG PET/CT for the prediction of outcome in patients with multiple myeloma. *J Nucl Med*. 2012;53:1829–35. <https://doi.org/10.2967/jnumed.112.106500>.
- McDonald JE, Kessler MM, Gardner MW, Buros AF, Ntambi JA, Waheed S, et al. Assessment of total lesion glycolysis by (18)F-FDG PET/CT significantly improves prognostic value of GEP and ISS in myeloma. *Clin Cancer Res*. 2017;23:1981–7. <https://doi.org/10.1158/1078-0432.ccr-16-0235>.
- Jung SH, Kwon SY, Min JJ, Bom HS, Ahn SY, Jung SY, et al. (18)F-FDG PET/CT is useful for determining survival outcomes of patients with multiple myeloma classified as stage II and III with the Revised International Staging System. *Eur J Nucl Med Mol Imaging*. 2019;46:107–15. <https://doi.org/10.1007/s00259-018-4114-0>.
- Zamagni E, Nanni C, Patriarca F, Englaro E, Castellucci P, Geatti O, et al. A prospective comparison of 18F-fluorodeoxyglucose positron emission tomography-computed tomography, magnetic resonance imaging and whole-body planar radiographs in the assessment of bone disease in newly diagnosed multiple myeloma. *Haematologica*. 2007;92:50–5.
- Spinnato P, Bazzocchi A, Brioli A, Nanni C, Zamagni E, Albinetti U, et al. Contrast enhanced MRI and (1)(8)F-FDG PET-CT in the assessment of multiple myeloma: a comparison of results in different phases of the disease. *Eur J Radiol*. 2012;81:4013–8. <https://doi.org/10.1016/j.ejrad.2012.06.028>.
- Nanni C, Zamagni E, Farsad M, Castellucci P, Tosi P, Cangini D, et al. Role of 18F-FDG PET/CT in the assessment of bone involvement in newly diagnosed multiple myeloma: preliminary results. *Eur J Nucl Med Mol Imaging*. 2006;33:525–31. <https://doi.org/10.1007/s00259-005-0004-3>.
- Rasche L, Angtuaco E, McDonald JE, Buros A, Stein C, Pawlyn C, et al. Low expression of hexokinase-2 is associated with false-

- negative FDG-positron emission tomography in multiple myeloma. *Blood*. 2017;130:30–4. <https://doi.org/10.1182/blood-2017-03-774422>.
10. Nanni C, Zamagni E, Versari A, Chauvie S, Bianchi A, Rensi M, et al. Image interpretation criteria for FDG PET/CT in multiple myeloma: a new proposal from an Italian expert panel. IMPeTUs (Italian Myeloma criteria for PET USe). *Eur J Nucl Med Mol Imaging*. 2016;43:414–21. <https://doi.org/10.1007/s00259-015-3200-9>.
 11. Philipp-Abbrederis K, Herrmann K, Knop S, Schottelius M, Eiber M, Luckerath K, et al. In vivo molecular imaging of chemokine receptor CXCR4 expression in patients with advanced multiple myeloma. *EMBO Mol Med*. 2015;7:477–87. <https://doi.org/10.15252/emmm.201404698>.
 12. Lapa C, Schreder M, Schirbel A, Samnick S, Kortum KM, Herrmann K, et al. [(68)Ga]Pentixafor-PET/CT for imaging of chemokine receptor CXCR4 expression in multiple myeloma - Comparison to [(18)F]FDG and laboratory values. *Theranostics*. 2017;7:205–12. <https://doi.org/10.7150/thno.16576>.
 13. Pan Q, Luo Y, Cao X, Ma Y, Li F. Multiple myeloma presenting as a superscan on 68Ga-Pentixafor PET/CT. *Clin Nucl Med*. 2018;43:462–3. <https://doi.org/10.1097/rlu.0000000000002067>.
 14. Rajkumar SV, Dimopoulos MA, Palumbo A, Blade J, Merlini G, Mateos MV, et al. International Myeloma Working Group updated criteria for the diagnosis of multiple myeloma. *Lancet Oncol*. 2014;15:e538–48. [https://doi.org/10.1016/s1470-2045\(14\)70442-5](https://doi.org/10.1016/s1470-2045(14)70442-5).
 15. Luo Y, Cao X, Pan Q, Li J, Feng J, Li F. (68)Ga-pentixafor PET/CT for imaging of chemokine receptor-4 expression in Waldenstrom macroglobulinemia/lymphoplasmacytic lymphoma: comparison to (18)F-FDG PET/CT. *J Nucl Med*. 2019. <https://doi.org/10.2967/jnumed.119.226134>.
 16. Nanni C, Versari A, Chauvie S, Bertone E, Bianchi A, Rensi M, et al. Interpretation criteria for FDG PET/CT in multiple myeloma (IMPeTUs): final results. IMPeTUs (Italian myeloma criteria for PET USe). *Eur J Nucl Med Mol Imaging*. 2018;45:712–9. <https://doi.org/10.1007/s00259-017-3909-8>.
 17. Greipp PR, San Miguel J, Durie BG, Crowley JJ, Barlogie B, Blade J, et al. International staging system for multiple myeloma. *J Clin Oncol*. 2005;23:3412–20. <https://doi.org/10.1200/jco.2005.04.242>.
 18. Palumbo A, Avet-Loiseau H, Oliva S, Lokhorst HM, Goldschmidt H, Rosinol L, et al. Revised international staging system for multiple myeloma: a report from International Myeloma Working Group. *J Clin Oncol*. 2015;33:2863–9. <https://doi.org/10.1200/jco.2015.61.2267>.
 19. Dolcino M, Patuzzo G, Barbieri A, Tinazzi E, Rizzi M, Beri R, et al. Gene expression profiling in peripheral blood mononuclear cells of patients with common variable immunodeficiency: modulation of adaptive immune response following intravenous immunoglobulin therapy. *PLoS One*. 2014;9:e97571. <https://doi.org/10.1371/journal.pone.0097571>.
 20. Alsayed Y, Ngo H, Runnels J, Leleu X, Singha UK, Pitsillides CM, et al. Mechanisms of regulation of CXCR4/SDF-1 (CXCL12)-dependent migration and homing in multiple myeloma. *Blood*. 2007;109:2708–17. <https://doi.org/10.1182/blood-2006-07-035857>.
 21. Stessman HA, Mansoor A, Zhan F, Janz S, Linden MA, Baughn LB, et al. Reduced CXCR4 expression is associated with extramedullary disease in a mouse model of myeloma and predicts poor survival in multiple myeloma patients treated with bortezomib. *Leukemia*. 2013;27:2075–7. <https://doi.org/10.1038/leu.2013.148>.
 22. Kyle RA, Rajkumar SV. Criteria for diagnosis, staging, risk stratification and response assessment of multiple myeloma. *Leukemia*. 2009;23:3–9. <https://doi.org/10.1038/leu.2008.291>.
 23. Cytawa W, Kircher S, Schirbel A, Shirai T, Fukushima K, Buck AK, et al. Chemokine receptor 4 expression in primary Sjogren's syndrome. *Clin Nucl Med*. 2018;43:835–6. <https://doi.org/10.1097/rlu.0000000000002258>.
 24. Derlin T, Gueler F, Brasen JH, Schmitz J, Hartung D, Herrmann TR, et al. Integrating MRI and chemokine receptor CXCR4-targeted PET for detection of leukocyte infiltration in complicated urinary tract infections after kidney transplantation. *J Nucl Med*. 2017;58:1831–7. <https://doi.org/10.2967/jnumed.117.193037>.
 25. Margaritopoulos GA, Antoniou KM, Lasithiotaki I, Prokrou A, Soufla G, Siafakas NM. Expression of SDF-1/CXCR4 axis in bone marrow mesenchymal stem cells derived from rheumatoid arthritis-usual interstitial pneumonia. *Clin Exp Rheumatol*. 2013;31:610–1.
 26. Wester HJ, Keller U, Schottelius M, Beer A, Philipp-Abbrederis K, Hoffmann F, et al. Disclosing the CXCR4 expression in lymphoproliferative diseases by targeted molecular imaging. *Theranostics*. 2015;5:618–30. <https://doi.org/10.7150/thno.11251>.
 27. Lapa C, Herrmann K, Schirbel A, Hanscheid H, Luckerath K, Schottelius M, et al. CXCR4-directed endoradiotherapy induces high response rates in extramedullary relapsed multiple myeloma. *Theranostics*. 2017;7:1589–97. <https://doi.org/10.7150/thno.19050>.
 28. Lapa C, Luckerath K, Kircher S, Hanscheid H, Grigoleit GU, Rosenwald A, et al. Potential influence of concomitant chemotherapy on CXCR4 expression in receptor directed endoradiotherapy. *Br J Haematol*. 2019;184:440–3. <https://doi.org/10.1111/bjh.15096>.

Publisher's note Springer Nature remains neutral with regard to jurisdictional claims in published maps and institutional affiliations.